JOURNAL OF CATALYSIS 130, 106–115 (1991)

Mechanistic Study of the Hydroformylation of Propene over Silica-Supported Rh and Pd Catalysts: Effect of Added Sodium Cation

SHUICHI NATIO*,[1] AND MITSUTOSHI TANIMOTO†

Research Centre for Spectrochemistry, Faculty of Science, The University of Tokyo, Hongo, Bunkyo-ku, Tokyo 113; and †Department of Chemistry, Faculty of Science, Shizuoka University, 836 Ohya, Shizuoka 422, Japan

Received April 2, 1990; revised February 25, 1991

The mechanism of the hydroformylation of propene over silica-supported Rh and Pd catalysts was studied by isotope tracer technique with microwave spectroscopy and infrared spectroscopic technique as well as kinetic investigation. The rate-determining steps in the hydroformylation process were different over the two metals: hydrogenation of surface acyl species on Rh catalysts and CO insertion into surface propyl species on Pd catalysts. The structure and the reactivity of the surface propyl intermediates were determined by analyzing the isotope distribution of monodeuteropropene formed during C_3H_6–D_2–CO reaction with microwave spectroscopy. It was revealed that *n*-propyl species is more reactive for CO insertion than *s*-propyl species. Promotion effect of sodium cations on hydroformylation was also investigated in detail and different roles of sodium cations were demonstrated for Rh and Pd catalysts.

INTRODUCTION

The mechanism of the hydroformylation of olefins by homogeneous transition-metal complexes has been studied extensively. Certain metal carbonyl complexes were identified as catalytically active reaction intermediates (*1–3*). However, the mechanism as well as the nature of active sites in the heterogeneous hydroformylation has not been clarified yet (*4–7*). Most of the heterogeneous systems studied so far are concerned with cation-exchanged Rh zeolite catalysts (*8–11*), where two completely different species have been proposed as the catalytically active species in the zeolite cage: Rh carbonyl complexes (*12*) and Rh metal particles (*13, 14*).

Metal cations such as Zn, Ti, and Fe have been reported to show an interesting promotion effect upon hydroformylation of ethene over silica-supported Rh metal catalysts, and the characteristic roles of the additives in the reaction were demonstrated (*15–17*). A similar promotion effect by alkali metal cations has been found in the CO–H_2 reaction over Pd (*18, 19*) and Rh (*20, 21*) metal catalysts. However, no investigations have been reported on the hydroformylation reactions. Recently we have investigated the hydroformylation of propene over silica-supported Rh, Pd, Pt, and Ni metal catalysts and found that all of them can catalyze this reaction to a large or small extent (*22*). The catalytic behavior was greatly dependent on the metal catalyst employed. Rh metal was the most selective catalyst for propene hydroformylation, while Pd metal was the most active catalyst even at lower reaction temperatures, although the selectivity for hydroformylation was only a few percent. We also studied the effect of added sodium cations and found a remarkable decrease in the activation energy for hydroformylation process.

In this paper we report on the mechanism of the hydroformylation of propene over silica-supported Rh and Pd catalysts. Since

[1] To whom correspondence should be addressed.

0021-9517/91 $3.00

these two metals exhibit different catalytic behavior mentioned above, it might be possible to clarify the factors controlling the activity and selectivity in this reaction by comparing the mechanistic difference between them. To investigate the details of the reaction pathway, we have conducted the C_3H_6–D_2–CO reaction as well as the C_3H_6–H_2–CO reaction. By observing the isotopic distribution patterns of monodeuteropropene formed in the hydrogen exchange process of propene by means of microwave spectroscopy, we can obtain information on the structure and the reactivity of adsorbed alkyl intermediates. We compare the kinetics and the reaction mechanisms for catalysts with and without added sodium cations and deduce their role in the hydroformylation process. Infrared spectroscopy is used to investigate the adsorbed state of CO and to obtain information on the electronic effect of sodium cations.

EXPERIMENTAL

Silica-supported Rh and Pd catalysts (5 wt%) were prepared by impregnating aqueous solutions of $RhCl_3$ and $PdCl_2$ onto SiO_2 (Aerosil 300, Nippon Aerosil, 300 m^2/g). To add sodium cations, Na_3RhCl_6 and Na_2PdCl_4 salts were employed. The catalyst powder (0.1–0.2 g) was placed in a U-shaped glass vessel, which was connected to a closed gas circulation system, and was reduced by hydrogen at 723 K for several hours. After the catalyst was evacuated for 0.5 h (base pressure: 1×10^{-5} Torr, 1 Torr = 133.3 $N\ m^{-2}$) and then cooled down to the room temperature, 50 Torr of CO was introduced into the system. The dispersion of the metals was determined from the adsorbed amount of CO: CO/Rh = 0.52 (Rh/SiO_2) and 0.40 (Rh–Na/SiO_2), CO/Pd = 0.082 (Pd/SiO_2), and 0.13 (Pd–Na/SiO_2).

H_2, D_2, and CO gases from commercial cylinders were passed over a heated Pd black catalyst to remove trace amounts of oxygen. C_3H_6 purchased from Takachiho Kagaku KK and C_3D_6 from Prochem were purified by a freeze–thaw cycle. The reaction was carried out in the same closed gas circulation system (total volume = ca. 300 cm^3) mentioned above. Before each run, the catalyst was reduced by 100 Torr of H_2 (or D_2) for 2 h at 573 K. After cooling to the reaction temperature, a certain amount of reaction gases was introduced into the system and the reaction was started, with a dry-ice–acetone cold trap to collect formed aldehyde and alcohol. The typical reaction condition was as follows: P_{H_2} = 100 Torr, P_{CO} = 50 Torr, and $P_{C_3H_6}$ = 25 Torr. A small amount (a few percent) of the circulating gas was sampled at a certain interval and analyzed by gas chromatography (molecular sieve 13X column for H_2 and CO, alumina column for propene and propane). At the same time, products collected in the cold trap were separated from the circulation system by a four-way stopcock and also analyzed by gas chromatography (PEG column). In the C_3H_6–D_2–CO reaction, deuterium contents in exchanged propene were determined with a mass spectrometer (Hitachi, RMU-6MG) using ionization voltage of 12 eV. The location of the deuterium atom in monodeuteropropene was determined by recording the microwave absorption line (1_{01}-0_{00} rotational transition) characteristic of each isotopic species. Details of the procedure were reported previously (*23, 24*). The notation for isotopomers in monodeuteropropene is

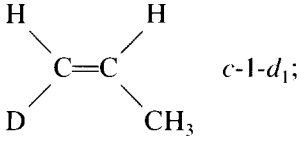

c-1-d_1;

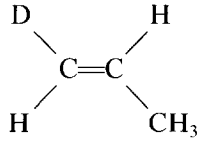

t-1-d_1;

CH_2=CD–CH_3, 2-d_1;

CH_2=CH–CH_2D, 3-d_1.

For infrared spectroscopic experiments, the catalysts were pressed into self-supporting disks (2 cm in diameter and 50–60 mg in

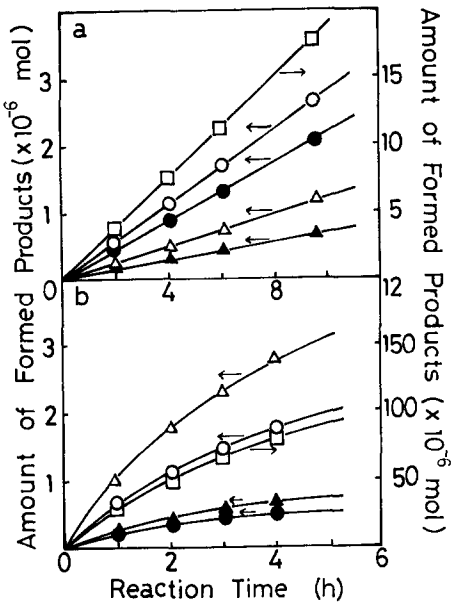

FIG. 1. Time course of C_3H_6–H_2–CO reaction over (a) Rh–Na/SiO_2 at 368 K and (b) Pd–Na/SiO_2 at 338 K. P_{H_2} = 100 Torr, P_{CO} Torr, and $P_{C_3H_6}$ = 25 Torr. (□) propane, (○) *n*-butyraldehyde, (●) *n*-butyl alcohol, (△) *s*-butyraldehyde, (▲) *s*-butyl alcohol.

weight). The catalyst disk was placed in an infrared cell, which was connected to a closed gas circulation system, and treated before the run in the same way as described above. Infrared spectra were measured at room temperature by a JASCO IRA-2 spectrometer.

RESULTS

Kinetic Study of C_3H_6–H_2–CO and C_3D_6–D_2–CO Reactions

Figure 1 demonstrates a typical example of the time profiles of C_3H_6–H_2–CO reactions over Rh–Na/SiO_2 and Pd–Na/SiO_2 catalysts. Hydrogenation and hydroformylation took place simultaneously, and propane, *n*- and *s*-butyraldehyde and *n*- and *s*-butyl alcohol were formed. The selectivity for these two processes greatly depended on the metal catalyst employed. Over Rh–Na/SiO_2 both hydrogenation and hydroformylation proceeded with similar rates, whereas over Pd–Na/SiO_2 the selectivity for the latter process was only a few percent of the former. Similar time profiles for C_3H_6–H_2–CO reactions were observed over Rh/SiO_2 and Pd/SiO_2 catalysts.

Table 1 summarizes the effect of added sodium cations upon the reaction rate as well as upon the regioselectivity. In the case of Rh catalysts both hydrogenation and hydroformylation processes were accelerated by sodium cations. On the other hand, over Pd catalysts the rate of hydroformylation was enhanced and that of hydrogenation suppressed. The addition of sodium cations did not change much the regioselectivity of the hydroformylation process: the ratio of *n*-isomers (*n*-butyraldehyde + *n*-butyl alcohol) to *s*-isomers (*s*-butyraldehyde + *s*-butyl alcohol) were 2.2–2.5 for Rh and Rh–Na catalysts and 0.4–0.5 for Pd and Pd–Na catalysts. The results for the C_3D_6–D_2–CO reaction are also listed in Table 1. Normal isotope effect (k_H/k_D = 1.0–1.5) was observed for the rate of propane formation, while fairly large inverse isotope effect (k_H/k_D = 0.5–0.8) was observed for the rate of hydroformylation. Little isotope effect was observed on the regioselectivity or on the ratio of aldehydes to alcohols formed during the hydroformylation reaction.

Temperature dependence of the turnover frequencies (TOF) of C_3H_6–H_2–CO and C_3D_6–D_2–CO reactions over these catalysts is demonstrated in Figs. 2 and 3. TOF was estimated using the value of metal dispersion obtained from the CO adsorption experiment. As mentioned above, both hydrogenation and hydroformylation processes were drastically accelerated by the addition of sodium cations over Rh catalysts (Fig. 2). Activation energies of these processes were lowered significantly by the sodium cation addition: for propane formation E_a = 97 kJ/mol (Rh) and 78 kJ/mol (Rh–Na), and for hydroformylation E_a = 57 kJ/mol (Rh) and 33 kJ/mol (Rh–Na). Figure 2 also demonstrates a large inverse isotope effect on the hydroformylation process, whereas no isotope effect was observed on the hydrogenation process. The bend at higher tem-

TABLE I

C_3H_6–H_2–CO and C_3D_6–D_2–CO Reactions over Various Catalysts

Catalyst	Reaction	Reaction rates ($\times 10^{-4}$ sec^{-1})		Regioselectivity (%)				Alcohol Aldehyde	n s
		$V_{propane}$	$V_{H\text{-}F}$	s-Ald	n-Ald	s-Alc	n-Alc		
Rh/SiO_2	I	6.3	3.5	15	40	15	31	0.84	2.4
	II	6.0	6.3	15	33	17	36	1.13	2.2
$Rh–Na/SiO_2$	I	38	12	10	35	19	36	1.22	2.4
	II	35	22	8	31	20	40	1.50	2.5
Pd/SiO_2	I	3.2	0.075	46	22	24	8	0.47	0.43
	II	2.1	0.099	44	20	24	12	0.56	0.47
$Pd–Na/SiO_2$	I	2.2	0.085	48	21	25	6	0.45	0.37
	II	2.2	0.18	50	20	22	8	0.43	0.39

Note. Reaction I: C_3H_6–H_2–CO. Reaction II: C_3D_6–D_2–CO. Reaction temperature: at 388 K over Rh/SiO_2 and $Rh–Na/SiO_2$, at 318 K over Pd/SiO_2 and $Pd–Na/SiO_2$. P(hydrogen) = 200 Torr, P(CO) = 50 Torr, P(propene) = 25 Torr.

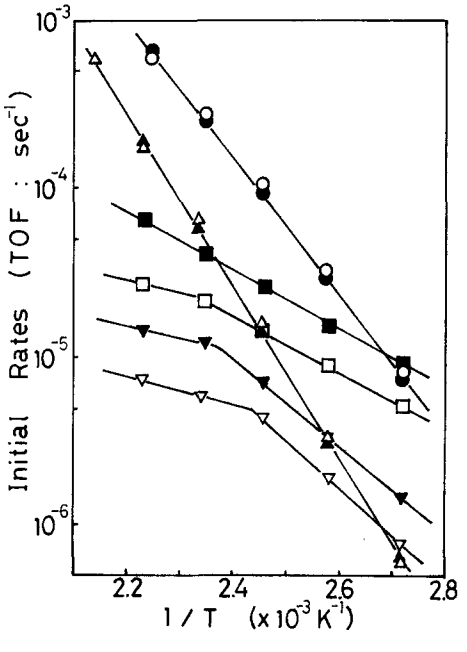

FIG. 2. Arrhenius plots of C_3H_6–H_2–CO and C_3D_6–D_2–CO reactions over $Rh–Na/SiO_2$ and Rh/SiO_2. P_{H_2} = 100 Torr, P_{CO} = 50 Torr, and $P_{C_3H_6}$ = 25 Torr. Open symbols: C_3H_6–H_2–CO. Closed symbols: C_3D_6–D_2–CO. (○●) propane (Rh–Na), (△▲) propane (Rh), (□■) hydroformylation (Rh–Na), (▽▼) hydroformylation (Rh).

peratures of the Arrhenius plot for the hydroformylation may be explained by the influence of the reverse reaction (decomposition of formed aldehyde and alcohol) in the catalyst bed. On the other hand, the activation energies of the hydrogenation process over Pd catalysts (Fig. 3) were not affected at all by the addition of sodium cations: E_a = 75 kJ/mol (Pd) and 74 kJ/mol (Pd–Na), although the turnover frequencies slightly decreased by the sodium addition. The activation energies for the hydroformylation process (Fig. 3) lowered significantly by the addition of sodium cations: E_a = 69 kJ/mol (Pd) and 36 kJ/mol (Pd–Na). Small normal isotope effect was observed in the hydrogenation process, whereas large inverse isotope effect was observed in the hydroformylation.

Pressure dependences of the turnover frequencies of the C_3H_6–H_2–CO reaction over $Rh–Na/SiO_2$ and $Pd–Na/SiO_2$ catalysts are summarized in Fig. 4. The reaction order, n, of hydroformylation as well as propane formation was fairly dependent on the metal catalysts employed, and the following empirical rate equations were derived:

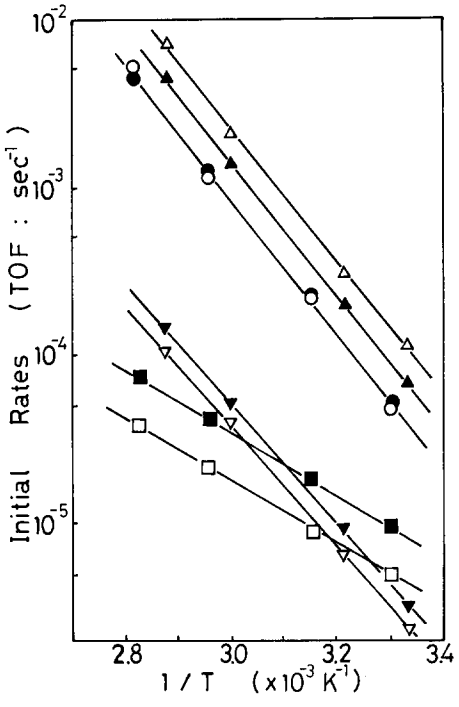

FIG. 3. Arrhenius plots of C_3H_6–H_2–CO and C_3D_6–D_2–CO reactions over Pd–Na/SiO_2 and Pd/SiO_2. P_{H_2} = 100 Torr, P_{CO} = 50 Torr, and $P_{C_3H_6}$ = 25 Torr. Open symbols: C_3H_6–H_2–CO. Closed symbols: C_3D_6–D_2–CO. (○●) propane (Pd–Na), (△▲) propane (Pd), (□■) hydroformylation (Pd–Na), (▽▼) hydroformylation (Pd).

$$\text{Rh–Na/SiO}_2;\quad V_{\text{propane}} = kP_{H_2}^{1.0}P_{CO}^{-1.3} \quad \text{and} \quad V_{\text{ald}} = k'P_{H_2}^{1.0}P_{CO}^{-0.3}.$$

$$\text{Pd–Na/SiO}_2:\quad V_{\text{propane}} = kP_{H_2}^{0.9}P_{CO}^{-0.9} \quad \text{and} \quad V_{\text{ald}} = k'P_{H_2}^{0.5}P_{CO}^{-0.2}.$$

Here, V_{propane} and V_{ald} represent the rate of the hydrogenation and hydroformylation process, respectively. In the former process, the reaction order for the partial pressure of carbon monoxide on Rh–Na/SiO_2 was more negative than that on Pd–Na/SiO_2, indicating stronger inhibition effect of adsorbed CO for the reaction. This may be the reason why the reaction proceeded at lower temperatures on Pd catalysts. However, in the latter process, the reaction order for the partial pressure of hydrogen on Rh–Na/SiO_2 was twice as large as that over Pd–Na/SiO_2, suggesting that the rate-determining steps are different for the two metals.

Microwave Spectroscopic Study of C_3H_6–D_2–CO Reaction

To obtain more information on the reaction intermediates and the mechanism, C_3H_6–D_2–CO reaction was investigated. Hydrogen exchange process of propene (V_e) proceeded more than one to two orders of magnitude faster than hydrogenation of propene (V_h), the ratio of the rates being: V_e/V_h = 110 (Rh), 120 (Rh–Na), 30 (Pd), and 50 (Pd–Na). Activation energies of this hydrogen exchange process were estimated to be about 100 kJ/mol (Rh) and 70 kJ/mol (Pd), which were similar to those of the hydrogenation process. Accordingly it is reasonable to suppose that both processes proceed via the same reaction intermediates, i.e., adsorbed *n*-propyl and *s*-propyl species (associative mechanism).

The microwave spectroscopic results on

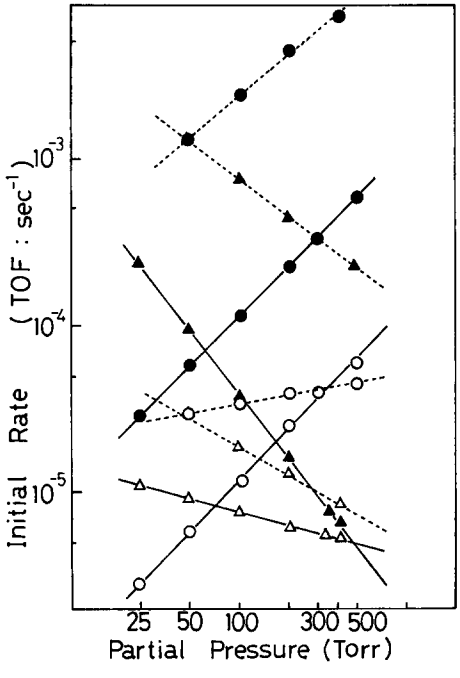

FIG. 4. Pressure dependence of the initial rates (TOF) of C_3H_6–H_2–CO reaction over Rh–Na/SiO_2 at 408 K, and over Pd–Na/SiO_2 at 338 K. Open symbols: hydroformylation. Closed symbols: propane formation. Solid line: Rh–Na. Broken line: Pd–Na. (○●) partial pressure of H_2 (P_{CO} = 50, $P_{C_3H_6}$ = 25 Torr), (△▲) partial pressure of CO (P_{H_2} = 100, $P_{C_3H_6}$ = 25 Torr).

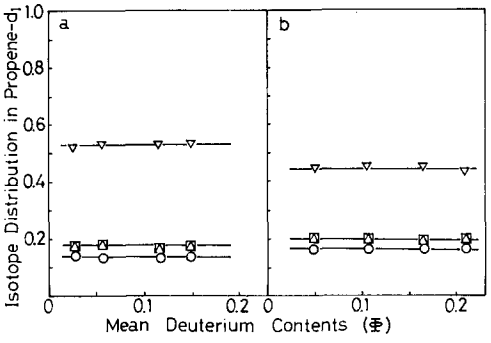

FIG. 5. Time course of the isotopic distribution in monodeuteropropene during C_3H_6–D_2–CO reactions at 453 K over (a) Rh–Na/SiO_2 and (b) Rh/SiO_2. (□) c-1-d_1, (▽) 2-d_1, (△) t-1-d_1, (○) 3-d_1 $\Phi = \frac{1}{6} * \Sigma_{i=0}^{6} i x[C_3H_{6-i}D_i]$: mean deuterium contents in propene.

the isotopic distribution of the monodeuteropropene formed by the hydrogen exchange process in the C_3H_6–D_2–CO reaction were displayed in Figs. 5 and 6. In the case of Rh/SiO_2 catalyst (Fig. 5(b)), the isotopic distribution pattern was 40% of propene-1-d_1, 44% of 2-d_1, and 16% of 3-d_1, which stayed constant during the reaction. Addition of sodium cations affected the distribution pattern slightly as shown in Fig. 5(a) (33% of propene-1-d_1, 54% of 2-d_1, and 13% of 3-d_1). In the associative mechanism, it is reasonable to suppose that propene-1-d_1 and 3-d_1 are formed through *s*-propyl intermediate and propene-2-d_1 through *n*-propyl intermediate. Accordingly, over Rh catalysts *n*-propyl adsorbed species is more reactive than *s*-propyl species in the hydrogen exchange process. If the two methyl groups of *s*-propyl adsorbed species are equivalent for hydrogen abstraction, the ratio of 1-d_1/3-d_1 will be $\frac{2}{3}$. However, the ratio in the present study ($\frac{40}{16}$ and $\frac{33}{13}$) is much larger than $\frac{2}{3}$, which suggests that the hydrogen exchange takes place mainly at the C_1 position of the double bond.

In contrast to the results on Rh/SiO_2 the isotope distribution on Pd/SiO_2 catalyst (Fig. 6(b)) changed considerably as the reaction proceeded. At the very beginning of the reaction, the main products were propene-*c*-1-d_1 and *t*-1-d_1, which decreased rapidly with the increase of propene-3-d_1, while propene-2-d_1 stayed unchanged in amount during the reaction. This pattern is quite similar to the one obtained in the C_3H_6–D_2 reaction over Pd/SiO_2 (*24*), which clearly indicates the existence of the intramolecular 1,3-hydrogen shift process after the deuterium incorporation through the associative mechanism. From the extrapolated values of the pattern into time zero (*c*- and *t*-1-d_1: 70%, 3-d_1: 20% and 2-d_1: 10%), it is recognized that *s*-propyl adsorbed species is much more reactive than *n*-propyl species for the deuterium incorporation process, which is definitely opposite to the result on Rh catalysts. Addition of sodium cations did not affect the isotopic distribution at all as shown in Fig. 6(a).

Infrared Spectroscopic Study of CO Adsorption and C_3H_6–H_2–CO Reaction

When CO was introduced over freshly reduced Rh/SiO_2 and Pd/SiO_2 catalysts, two main peaks were observed as summarized in Table 2, which agreed well with the frequencies reported in the literature (*19, 25, 26*). A strong band at wavenumber higher than 2000 cm^{-1} can be assigned to linear CO(a) and a broadband at around 1900–1800 cm^{-1} to bridged CO(a). On addition of sodium cations over Rh/SiO_2 and Pd/SiO_2 cat-

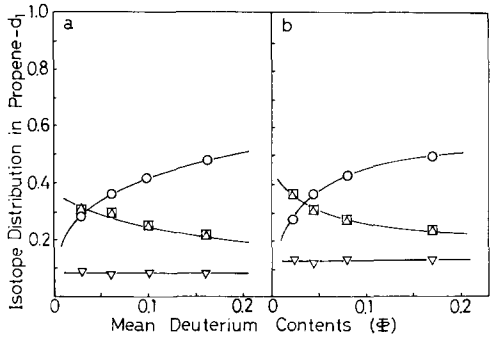

FIG. 6. Time course of the isotopic distribution in monodeuteropropene during C_3H_6–D_2–CO reactions at 318 K over (a) Pd–Na/SiO_2 and (b) Pd/SiO_2. (□) c-1-d_1, (△) t-1-d_1, (▽) 2-d_1, (○) 3-d_1.

TABLE 2

Infrared Spectra of Adsorbed CO

Catalysts	Wavenumbers (cm^{-1}) of CO(a)			
	CO only at 298 K		C_3H_6–H_2–CO at 423 K	
	Linear	Bridge	Linear	Bridge
Rh/SiO_2	2073	1915	2071	1915
Rh–Na/SiO_2	2055	1830	2038	1794
Pd/SiO_2	2075	1985	2075	1975
Pd–Na/SiO_2	2060	1855	2055	1790

alysts, the peak positions of the linear as well as the bridge bands shifted to the lower wavenumbers by 15–20 and 90–150 cm^{-1}, respectively. These results indicate that the electronic states of Rh and Pd surface metal atoms were considerably modified by the sodium cation addition.

When the mixture of C_3H_6 and H_2 was added to the CO-preadsorbed surfaces at room temperature, the intensity of CO(a) bands remained unchanged, indicating that CO is adsorbed much stronger than propene and hydrogen. Most of the surface may be thus covered by CO(a). During the C_3H_6–H_2–CO reaction at 423 K, the CO(a) bands did not shift at all over Rh/SiO_2 and Pd/SiO_2 catalysts. Over sodium-added catalysts, however, the bridged CO(a) bands shifted toward the lower wavenumbers by 40–60 cm^{-1} during the reaction. As the reaction proceeded, several complex bands emerged, which might be assigned to adsorbed butyraldehyde and butyl alcohol, formed by the hydroformylation process.

DISCUSSION

Reaction Mechanism of Hydroformylation

The microwave spectrocopy is a powerful technique to investigate the structure of the reaction intermediates in the C_3H_6–D_2 reaction by observing the isotopic distribution of monodeuteropropene formed in the hydrogen exchange process. In the C_3H_6–D_2–CO reactions in the present study, the relative activity of *n*-propyl and *s*-propyl intermediates in the hydrogen exchange process could be estimated by this method. In addition, if both of them are reaction intermediates also for the hydrogormylation process, it may be possible to estimate the relative reactivity of the adsorbed alkyl species for the hydroformylation process by analyzing microwave spectroscopic data.

The product ratios of *n*-isomers(butyraldehyde + butyl alcohol) to *s*-isomers in Table 1 clearly indicate that *n*-propyl species are more reactive than *s*-propyl species for the hydroformylation process on Rh catalysts, whereas the situation is opposite on Pd catalysts. The activity ratios of the propyl intermediates well correspond to those for the hydrogen exchange process obtained from Figs. 5 and 6. Accordingly, the assumption mentioned above is applicable in this case, that is, hydrogenation and hydroformylation proceed through the common alkyl intermediates on the catalysts employed in this study.

Since propane, butyraldehyde and butyl alcohol were the only products detected during the reaction, it is necessary to consider hydrogenation and hydroformylation of propene alone. Accordingly, we assume a simple but generally accepted reaction scheme for this reaction:

$$H_2 + 2S \overset{K_1}{\rightleftharpoons} 2H_S \qquad \text{step 1}$$

$$CO + S \overset{K_2}{\rightleftharpoons} CO_S \qquad \text{step 2}$$

$$C_3H_6 + S \overset{K_3}{\rightleftharpoons} C_3H_{6S} \qquad \text{step 3}$$

$$C_3H_{6S} + H_S \overset{K_4}{\rightleftharpoons} C_3H_{7S} + S \qquad \text{step 4}$$

$$C_3H_{7S} + CO_S \overset{K_5(k_5)}{\rightleftharpoons\!\!\rightarrow} C_4H_7O_S + S \qquad \text{step 5}$$

$$C_4H_7O_S + H_S \overset{k_6}{\rightarrow} C_4H_8O + S \qquad \text{step 6}$$

$$C_3H_{7S} + H_S \overset{k_7}{\rightarrow} C_3H_8 + S \qquad \text{step 7}$$

In the above scheme S is a surface vacant

site and the suffix S shows that the species is a surface-adsorbed species. K_1–K_5 represent the equilibrium constants of the corresponding steps, and k_5, k_6, and k_7 the rate constants of the forward reaction of the respective steps. It is reasonable to suppose that adsorption steps of the reactants (steps 1–3) are in equilibrium. From the results of the C_3H_6–D_2–CO reaction, hydrogen exchange process of propene is recognized to be one to two orders of magnitude faster than hydrogenation and hydroformylation of propene, suggesting the equilibrium in step 4. As discussed already, steps 5 and 7, which proceed competitively through the common adsorbed propyl intermediates, determine the selectivity of the reaction.

According to the above reaction scheme, the coverage of each adsorbed species during the reaction can be expressed as follows:

$$\Theta_S = 1/\{1 + (K_1P_{H_2})^{0.5} + K_2P_{CO} + K_3P_P\},$$

$$\Theta_H = \Theta_S(K_1P_{H_2})^{0.5}, \quad \Theta_{CO} = \Theta_S K_2 P_{CO}, \quad P_P = \Theta_S K_3 P_P,$$

$$\Theta_{C_3H_7} = \Theta_S(K_1)^{0.5}K_3K_4(P_{H_2})^{0.5}P_P,$$

where P_P, P_{H_2}, P_{CO}, and Θ_P, Θ_H, Θ_{CO}, Θ_S represent the partial pressure (P) and coverage (Θ) of propene, hydrogen, CO, and vacant sites. The rate-determining step of propane formation should be step 7, and the rate for propane formation is hence given by

$$V_{propane} = k_7\Theta_{C_3H_7}\Theta_H = k_7K_1K_3K_4P_{H_2}P_P/\{1 + (K_1P_{H_2})^{0.5} + K_2P_{CO} + K_3P_P\}^2. \quad (1)$$

On the other hand, two different rate-determining steps would be possible for the aldehyde formation. If the CO insertion (step 5) is the rate-determing step, the rate equation for butyraldehyde formation is

$$V_{ald} = k_5\Theta_{C_3H_7}\Theta_{CO} = k_5(K_1)^{0.5}K_2K_3K_4(P_{H_2})^{0.5}P_{CO}P_P/\{1 + (K_1P_{H_2})^{0.5} + K_2P_{CO} + K_3P_P\}^2. \quad (2)$$

If the step 5 is in equilibrium (K_5) and the step 6 determines the rate, the coverage of the acyl intermediates and the rate of butyraldehyde formation can be expressed as

$$\Theta_{C_3H_7O} = \Theta_S(K_1)^{0.5}K_2K_3K_4K_5(P_{H_2})^{0.5}P_PP_{CO}$$

$$V_{ald} = k_6\Theta_{C_3H_7O}\Theta_H = k_6K_1K_2K_3K_4K_5P_{H_2}P_{CO}P_P/\{1 + (K_1P_{H_2})^{0.5} + K_2P_{CO} + K_3P_P\}^2. \quad (3)$$

Comparison of Eqs. (1)–(3) allows following predictions for the dependence on hydrogen partial pressure. When hydrogenation of the acyl group (step 6) is the rate-determining step, both rates of propane and aldehyde formations exhibit the same dependence upon the hydrogen partial pressure. When CO insertion (step 5) is rate-determining, however, hydrogen pressure dependence of aldehyde formation should be significantly smaller than that of propane formation.

From the rate equations as described in Results, the reaction orders with respect to the partial pressure of hydrogen are: $n_{propane} = 0.9$ and $n_{ald} = 0.5$ for Pd–Na/SiO_2, and $n_{propane} = n_{ald} = 1.0$ for Rh–Na/SiO_2. These results clearly indicate that CO insertion is the rate-determining step in hydroformylation on palladium catalyst, while hydrogenation of the acyl intermediate is rate-determining on rhodium catalyst. In the catalysis by homogeneous Rh carbonyl complexes, it has been generally accepted that CO insertion is fast and that the subsequent hydrogenation of acyl intermediate is the rate-determining step. This is valid also for heterogeneous rhodium catalyst (*3*). On the other hand, palladium carbonyl complexes are less active for CO insertion in homogeneous catalytic system (*3*), which is in accordance with the present result.

Estimation of Relative Activity of n- and s-propyl Species

By using the rate equations, it is possible to estimate the relative activity of *n*-propyl and *s*-propyl intermediates for the hydroformylation process. As discussed above, selectivity for hydrogenation and hydroformylation is determined by the ratio of the reaction rates of step 5 and 7. On the other hand, the regioselectivity in the hydrofor-

mylation process may be determined by the ratio of the surface concentrations of *n*-propyl and *s*-propyl intermediates, which can be estimated from the microwave spectroscopic analysis of the monodeuteropropenes formed through the reverse reaction of step 4 in the C_3H_6–D_2–CO reaction. In the reverse process of step 4, the rates of propene-2-d_1 and propene-1-d_1 + 3-d_1 formation can be written as

$$V_{2-d_1} = k^n_{-4}\Theta_{n-C_3H_7} * \Theta_S, \quad (4)$$

$$V_{1-d_1+3-d_1} = k^s_{-4}\Theta_{s-C_3H_7} * \Theta_S.$$

On the other hand, the rates of *n*- and *s*-butyraldehyde formation over Rh catalyst can be expressed as

$$V_{n-ald} = k^n_6\Theta_{n-C_3H_7O} * \Theta_H = k^n_6K^n_5\Theta_{n-C_3H_7} * \Theta_{CO} * \Theta_H * \Theta_S^{-1},$$

$$V_{s-ald} = k^s_6\Theta_{s-C_3H_7O} * \Theta_H = k^s_6K^s_5\Theta_{s-C_3H_7} * \Theta_{CO} * \Theta_H * \Theta_S^{-1}. \quad (5)$$

At the initial stage of the reaction, the ratio of these rate equations can be given by the ratio of the products concentration,

$$V_{2-d_1}/V_{1-d_1+3-d_1} = [\text{propene-2-}d_1]/[\text{propene-1-}d_1 + \text{propene-3-}d_1],$$

$$V_{n-ald}/V_{s-ald} = [n\text{-butyraldehyde}]/[s\text{-butyraldehyde}],$$

and hence,

$$[n\text{-butyraldehyde}]/[s\text{-butyraldehyde}] = (k^n_6K^n_5/k^s_6K^s_5) * (k^s_{-4}/k^n_{-4}) * [\text{propene-2-}d_1]/[\text{propene-1-}d_1 + \text{propene-3-}d_1]. \quad (6)$$

For the reactions over Pd catalyst similar relation can be derived. It takes the same form as Eq. (6) above, if $k^n_6K^n_5$ and $k^s_6K^s_5$ should be replaced by k^n_5 and k^s_5.

From Table 1 and Figs. 5 and 6, the average values of the ratios of the products are

$$[n\text{-butyraldehyde}]/[s\text{-butyraldehyde}] = 2.5(\text{Rh}) \text{ and } 0.4(\text{Pd})$$

$$[\text{propene-2-}d_1]/[\text{propene-1-}d_1 + \text{propene-3-}d_1] = 0.8(\text{Rh}) \text{ and } 0.15(\text{Pd}).$$

By introducing these values into Eq. (6), the following relation can be derived:

$$k^n_6K^n_5/k^s_6K^s_5 = k^n_{-4}/k^s_{-4} \times 3.1 \quad \text{(for the reaction over Rh)},$$

$$k^n_5/k^s_5 = k^n_{-4}/k^s_{-4} \times 2.7 \quad \text{(for the reaction over Pd)}.$$

These relations indicate that over Pd catalyst activity ratios of *n*-propyl to *s*-propyl species for CO insertion process to form butyraldehydes is about three times larger than that for hydrogen abstraction process to form propene. The situation is not so clearcut in the case of Rh catalysts, but similar conclusions may be derived from the results mentioned above. This conclusion is reasonable if we consider larger steric influence of *s*-propyl for CO insertion or *s*-butyryl intermediate for hydrogen addition. It is interesting to note that the activation energies for the formation of the corresponding aldehydes are not so different from each other.

Effect of Sodium Cation Addition

Addition of sodium cations to Rh catalysts increased the TOF and decreased the activation energy of the hydrogenation process, with 20% increase in the ratio [propene-2-d_1]/[propene-1-d_1 + 3-d_1]. On the other hand, the activation energy of the propane formation over Pd catalysts remained almost unchanged by the sodium cation addition. TOF decreased slightly and the ratio of [propene-2-d_1]/[propene-1-d_1 + 3-d_1] did not change at all. As far as infrared spectra are concerned (Table 2), addition of sodium cations causes similar electronic modification in Rh and Pd catalysts. It is not clear why sodium cations influence the hydrogenation reaction differently over these catalysts.

The effect of the sodium cation addition on the hydroformylation is the increase in

TOF and the decrease in activation energies over both Pd and Rh catalysts. Since CO insertion into and hydrogenation of acyl intermediates are the rate-determining steps of this reaction on Pd and Rh, respectively, sodium cation must promote the reaction in a different way for each metal.

Similar promotion effect was observed on the oxygenated compound formation in $CO-H_2$ reactions over Pd/SiO_2 catalysts (*18, 19*). Without sodium cations, the main product was methane with a smaller amount of methanol. The addition of sodium cation changed neither TOF nor activation energy of methane formation (105 kJ/mol). However, for methanol formation, activation energy decreased from 84 to 75 kJ/mol and TOF increased by one order of magnitude. Infrared spectroscopic investigation as well as application of isotope tracer technique revealed that formyl intermediates were stabilized as surface formate ions to facilitate methanol formation under mild conditions. The role of added sodium cations was to supply surface oxygen atoms available for formate formation (*25*). Accordingly, it is reasonable to suppose that similar stabilization of acyl intermediate such as butyrate ion as well as the promotion effect in CO insertion process plays an important role in the reaction studied here.

On the other hand, the promotion effect of sodium cation addition was not observed on the C_2-oxygenated compound formation in $CO-H_2$ reaction over Rh/SiO_2 catalysts (*26*). The marked promotion effect observed in the present hydroformylation reaction on $Rh-Na/SiO_2$ catalyst can be explained by the different rate-determining steps in these two reactions.

REFERENCES

1. Edans, D., Osborn, J. A., and Wilkinson, G., *J. Chem. Soc. A*, 3133 (1968).
2. Brown, C. K. and Wilkinson, G., *J. Chem. Soc. A*, 2753 (1970).
3. Cornils, B., *In* "New Synthesis with Carbon Monoxide" (J. Falbe, Ed.), pp. 1–181. Springer-Verlag, Berlin/New York, 1988.
4. Arai, H., Kaneko, T., and Kunugi, T., *Chem. Lett.*, 265 (1975).
5. Arai, H., *J. Catal.* **51,** 135 (1978).
6. Ichikawa, M., *J. Catal.* **59,** 67 (1979).
7. Kobayashi, M., *Chem. Lett.*, 1215 (1984).
8. Arai, H. and Tominaga, H., *J. Catal.* **75,** 188 (1982).
9. Takahashi, N. and Kobayashi, M., *J. Catal.* **85,** 89 (1984).
10. Davis, M. E., Rode, E., Taylor, D., and Hanson, B. E., *J. Catal.* **86,** 67 (1984).
11. Davis, R. J., Rossin, J. A., and Hanson, B. E., *J. Catal.* **98,** 477 (1986).
12. Rode, E. J., Davis, M. E., and Hanson, B. E., *J. Catal.* **96,** 563 and 574 (1985).
13. Denley, D. R., Raymond, R. H., and Tang, S. C., *J. Catal.* **87,** 414 (1984).
14. Takahashi, N., Mijin, A., Suematsu, H., Shinohara, S., and Matsuoka, H., *J. Catal.* **117,** 348 (1989).
15. Ichikawa, M., Fukushima, T., and Shikakura, K., *in* "Proceedings, 8th International Congress on Catalysis, Berlin, 1984," Vol. 2, p. 69. Dechema, Frankfurt-Am-Main, 1984.
16. Ichikawa, M., Lang, A. J., Shriver, D. F., and Sachtler, W. M. H., *J. Am. Chem. Soc.* **107,** 7216 (1985).
17. Sachtler, W. M. H., and Ichikawa, M., *J. Phys. Chem.* **90,** 4752 (1986).
18. Kikuzono, Y., Kagami, S., Naito, S., Onishi, T., and Tamaru, K., *Chem. Lett.*, 1249 (1981).
19. Kikuzono, Y., Kagami, S., Naito, S., Onishi, T., and Tamaru, K., *J. Chem. Soc., Faraday Disc.*, 135 (1981).
20. Kagami, S., Naito, S., Kikuzono, Y., and Tamaru, K., *J. Chem. Soc. Chem. Comm.*, 256 (1983).
21. Orita, H., Naito, S., and Tamaru, K., *Chem. Lett.*, 1161 (1983).
22. Naito, S., and Tanimoto, M., *J. Chem. Soc. Chem. Commun.*, 1403 (1989).
23. Naito, S., and Tanimoto, M., *J. Chem. Soc., Faraday Trans. 1* **84,** 4115 (1988).
24. Naito, S., and Tanimoto, M., *J. Catal.* **102,** 377 (1986).
25. Naito, S., Yoshioka, H., Orita, H., and Tamaru, K., *in* "Proceedings, 8th International Congress on Catalysis, Berlin, 1984," Vol. 2, p. 207. Dechema, Frankfurt-am-Main, 1984.
26. Orita, H., Naito, S., and Tamaru, K., *J. Catal.* **90,** 183 (1984).